Enhancing Nearfield Acoustic Holography using Wavelet Transform

Byeongsik Ko*

Director, Korea simulation technology Inc.
Wonyoung B/D 362-11, Hapjeong-Dong, Mapo-Gu, Seoul, Korea

When there are low signal to noise relationships or low coherences between measured pressure and a reference sensor, a pressure field measured and estimated by NAH (Nearfield Acoustic Holography) becomes noisy on the hologram and source planes. This paper proposes a method to obtain the high coherent de-noised pressure signals from low coherent noisy ones by combining a wavelet algorithm with NAH. The proposed method obtains the de-noised field from acoustic fields on a noise source plane reconstructed through backward propagation of NAH. Thus this method does not need high coherent pressure signals on the hologram surface while the conventional nearfield acoustic holography requires high-coherent signals. The proposed method was verified by numerical simulation using noisy signals, composed of original signals and imposed noises distributed on the hologram surface.

1. Introduction

In practical noise engineering applications, it is often required to reconstruct noise sources as an inverse problem so as to come up with better designs to reduce resulting noise suppression. In case of an inverse acoustic radiation problem, it is to determine the acoustic quantities on the source surface based on measured acoustic pressure signals in the field.

There had been many investigations for identifying or visualizing noise sources. Identification of noise sources is very important because one can control the noise after finding noise sources in the system such as the interior cabin of a vehicle or an aircraft. Acoustic holography method is one of the best schemes for identifying and visualizing an acoustic field. The quality of the hologram depends strongly upon the size of the hologram

surface, its microphone spacing, the spatial resolution, the disturbance including the incorrect position of the microphones, and the environment like an anechoic chamber.

Disturbances or errors appeared on the hologram surface significantly affect the quality of the acoustic field that will be reconstructed on the source surface. In this paper a methodology for enhancing the acoustic field image will be developed using NAH and a wavelet.

Identification of the acoustic field was initiated from imaging schemes formulated as optical holography equations, which can be found in Goodman (1968). NAH can be used to get the source position at the surface, or to determine how the sound field propagates from the surface and into the farfield. The advantages of NAH include the consistent spatial data sets, the possibility of an automated measurement process, the evaluation of transient or steady state noise sources, and the availability of 3D acoustic quantities. Inverse acoustics using NAH, which is proposed by Maynard (1985), Verosi et. al. (1987) and Wang (1997), has been the subject of extensive studies for the past two decades and has been

* E-mail : bs_ko@hotmail.com
  TEL : +82-2-3775-0051; FAX : +82-2-3775-0054
  Director, Korea simulation technology Inc. Wonyoung B/D 362-11, Hapjeong-Dong, Mapo-Gu, Seoul, Korea.
  (Manuscript **Received** December 22, 2003; **Revised** July 1, 2004)

investigated in many areas by several researchers like Maynard(1985), Verosi et. al.(1987), Wang and Wu(1997), Dumbacher(2000), Borgiotti (1990).

Wavelet analysis was initiated by Alfred Haar (1910) and the concept of wavelets in theoretical form was first proposed by Jean Morlet(1983). The methods of wavelet analysis have been mainly developed by Y. Meyer(1993). The wavelet transform has become a standard tool in signal and image processing, and it has found applications to almost all fields of physics, engineering and applied mathematics. There are many practical applications for de-noising including image, video quality enhancement and even astronomy and astrophysics for studying solar corona and detection of gamma sources. Said and Peralman(1996) Shapiro(1993) reported that the discrete WT is more appropriate for signal compression and reconstruction, and it is especially popular in the signal processing community. De-noising using the wavelet is used to produce enhanced estimates of an image corrupted by noise. The restored image should contain less noise than the original noisy one and be sharp. Chambolle(1998), Chang and Vetterli (1997), Coifman and Donoho(1995), Donoho (1992, 1994, 1995), Shao and Cherkassky(1998) reported that it means that de-noising should result in sharpening the edges of the original noisy image. One of the key properties underlying the success of wavelets is that the wavelet transform provides excellent localization in both time and frequency domain. In addition, wavelet expansions tend to concentrate the signal energy within a relatively small number of (large) coefficients.

Simoncelli(1999) reported de-noising can be viewed as a signal estimation problem in which one wants to estimate the original (noise-free) image signal from the noisy samples. The wavelet thresholding method originally proposed by Donoho(1992, 1994, 1995), is a signal estimation technique that exploits remarkable abilities of wavelet transform for signal de-noising and compression. It removes noise by discarding coefficients that are insignificant relative to some threshold (assuming that the small coefficients are mainly contributed by the additive noise). Coifman and Donoho (1995), Donoho(1994, 1995) reported that wavelet thresholding solution is asymptotically optimal in a minimax MSE (Mean Squared Error) sense over a variety of smoothness spaces.

Wavelet transform represents the image signal as a superposition of wavelet basis functions (or the wavelet basis images) weighted by the corresponding wavelet coefficients. Since wavelet transform uses orthogonal basis functions, the wavelet coefficients can be computed easily by orthogonal decomposition. When using a subset of wavelet basis functions to approximate the original signal, we do not need to re-compute the corresponding subset of coefficients.

This paper is mainly concerned with an inverse acoustics using NAH and wavelet analysis. The acoustic field on the noise source surface is reconstructed from measured acoustic pressure signals on a hologram surface. When there are low coherences between measured pressure and the reference sensor, a pressure field measured and estimated by NAH (Nearfield Acoustic Holography) has a noisy acoustic field on source plane. It is caused by low coherences between measured pressure and the reference sensor on a hologram surface or by low signal-to-noise ratio.

This paper proposes a method to get the clear acoustic field from a noisy one by combining a wavelet algorithm with NAH. The proposed method obtains the de-noised field from a noisy field on a noise source plane reconstructed through backward propagation of NAH.

2. Theory

There are several algorithms for identifying noise sources, which are beam-forming method and nearfield acoustic holography. Nearfield acoustic holography has been developed by Maynard et. al (1985, 1987) since the mid of 1980. Many researchers have developed an NAH algorithm for enhancing NAH performance hereafter. But the main obstacles for testing NAH are to measure the noise inside an anechoic

chamber or a semi-anechoic chamber and to utilize high-end microphones with high signal-to-noise ratio. Measuring the noise inside an anechoic chamber is the ideal solution for obtaining a clear image on a hologram surface.

2.1 Nearfield acoustic holography

The linearized homogeneous wave equation can be expressed as follows :

$$\nabla^2 p_{(\mathbf{x},t)} - \frac{1}{c^2}\frac{\partial^2 p_{(\mathbf{x},t)}}{\partial t^2} = 0 \qquad (1)$$

where $p_{(\mathbf{x},t)}$ is the pressure at position $\mathbf{x}$ and is the speed of sound. The time domain can be transformed into the frequency domain by using the Fourier transform as follows :

$$P_{(\mathbf{x},\omega)} = F_T\{p_{(\mathbf{x},t)}\} = \int_{-\infty}^{\infty} p_{(\mathbf{x},t)} e^{j\omega t} dt \qquad (2)$$

$$p_{(\mathbf{x},t)} = F_T^{-1}\{P_{(\mathbf{x},\omega)}\} = \frac{1}{2\pi}\int_{-\infty}^{\infty} P_{(\mathbf{x},\omega)} e^{-j\omega t} d\omega \qquad (3)$$

where F_T and denote F_T^{-1} the Fourier transform and inverse Fourier transform with respect to time.

The wave equation with harmonic motion can be obtained from the Fourier transform

$$\nabla^2 P_{(\mathbf{x},\omega)} + k^2 P_{(\mathbf{x},\omega)} = 0 \qquad (4)$$

where $P_{(\mathbf{x},\omega)}$ is the complex pressure and $k = \frac{\omega}{c}$ is the wave number of the sound field. According to the Helmholtz integral equation, the solution can be expressed as :

$$P_{(\mathbf{x},\omega)} = \frac{1}{4\pi}\iint_S \left(jk\rho_0 c V_{n(\boldsymbol{\xi},\omega)} G_{(\mathbf{x}|\boldsymbol{\xi},\omega)} - P_{(\boldsymbol{\xi},\omega)}\frac{\partial G_{(\mathbf{x}|\boldsymbol{\xi},\omega)}}{\partial n}\right) d\boldsymbol{\xi} \quad (5)$$

where ρ_0 is the density of the medium and $P_{(\mathbf{x},\omega)}$ is the pressure at position x at frequency ω, and $P_{(\boldsymbol{\xi},\omega)}$ and $V_{n(\boldsymbol{\xi},\omega)}$ are the pressure and the velocity component normal to boundary surface S. $G_{(\mathbf{x}|\boldsymbol{\xi},\omega)}$ denotes the Green's function and $\boldsymbol{\xi}$ represents the position of acoustic source.

In practice, the Green function G is known provided that the part of S not at infinity is the level surface of a separable coordinate system. The three spatial coordinates of source surface are expressed as ξ_1, ξ_2 and ξ_3, with the level surface
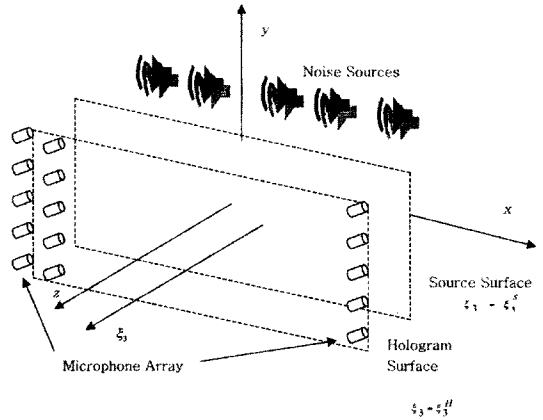
Fig. 1 Coordinate system in Nearfield Acoustic Holography

given by $\xi_3 = \xi_3^S$. The hologram surface is given by $\xi_3 = \xi_3^H$, where the constant $\xi_3^H > \xi_3^S$ (Fig. 1).

If $G_{(\mathbf{x}|\boldsymbol{\xi},\omega)}$ satisfies the homogeneous Dirichlet boundary condition on the source plane, Eq. (5) will be simplified since the first term in Eq. (5) will be eliminated. In Cartesian coordinate system, the Green's function can be constructed with the homogeneous boundary condition. Since it is assumed that $G_{(\mathbf{x}|\boldsymbol{\xi},\omega)}$ satisfies the homogeneous Dirichlet condition on the surface is known, then Eq. (5) becomes :

$$P_{(\xi_1,\xi_2,\xi_3)} = \iint P_{(\xi_1',\xi_2',\xi_3^S)} G_{HS(\xi_1-\xi_1',\xi_2-\xi_2',\xi_3-\xi_3^S)} d\xi_1' d\xi_2' \quad (6)$$

where $G_{HS(\xi_1-\xi_1',\xi_2-\xi_2',\xi_3-\xi_3^S)}$ is the transformation regarding to the wave propagation and is denoted by $G_{HS(\xi_1-\xi_1',\xi_2-\xi_2',\xi_3-\xi_3^S)} = \frac{\partial G_{(\mathbf{x}|\boldsymbol{\xi},\omega)}}{\partial n}$, normal derivative of Green's function.

The above equation denotes the convolution form.

But this cannot be evaluated directly because the acoustic field is known or measured on a hologram surface, not on a source surface. If Eq. (7) is evaluated for $\xi_3 = \xi_3^H$ the following relationship can be obtained :

$$P_{(\xi_1,\xi_2,\xi_3^H)} = \iint P_{(\xi_1',\xi_2',\xi_3^S)} G_{(\xi_1-\xi_1',\xi_2-\xi_2')} d\xi_1' d\xi_2' \quad (7)$$

The RHS term of Eq. (8) is a two-dimensional convolution ; By using the convolution theorem,

Eq. (8) can be inverted to obtain $P_{(\xi_1,\xi_2,\xi_3')}$ in terms of $P_{(\xi_1,\xi_2,\xi_3')}$. Denoting a two-dimensional spatial Fourier transform, or a wavenumber transform, by F and its inverse by F^{-1},

$$\hat{P}_{(k_x,k_y,z;\omega)}=F\{\,P_{(x,y,z;\omega)}\}$$
$$=\int_{-\infty}^{\infty}\int_{-\infty}^{\infty}P_{(x,y,z;\omega)}e^{-j(k_xx+k_yy)}\,dxdy \quad (8)$$

$$P_{(x,y,z;\omega)}=F^{-1}\{\,\hat{P}_{(k_x,k_y,z;\omega)}\}$$
$$=\int_{-\infty}^{\infty}\int_{-\infty}^{\infty}P_{(k_x,k_y,z;\omega)}e^{j(k_xx+k_yy)}\,dx_xdy_y \quad (9)$$

These transformations map functions from space domain to wavenumber domain and vice versa. By the use of the reconstructive equation expressed as a convolution,

$$\hat{P}_{(k_x,k_y,z;\omega)}=\hat{G}_{HS(k_x,k_y,z-z_s;\omega)}P_{(k_x,k_y,z_s;\omega)} \quad (10)$$

where

$$\hat{G}_{HS(k_x,k_y,z-z_s;\omega)}=F\{\,G_{HS(x,y,z-z_s;\omega)}\}=e^{jk_z(z-z_s)}$$

and $k_z=\sqrt{k^2-k_x^2-k_y^2}$ is the z-directional wavenumber.

By combining all the equations to reconstruct the acoustic field on an arbitrary position, the reconstructive field can be expressed as follows :

$$P_{(x,y,z;\omega)}=F^{-1}\{\hat{G}_{HS(k_x,k_y,z-z_s;\omega)}\hat{P}_{(k_x,k_y,z_s;\omega)}\} \quad (11)$$

Similarly, the acoustic field on a source surface can be expressed in terms of that on a hologram surface as follows :

$$P_{(x,y,z_s;\omega)}=F^{-1}\{\hat{G}_{HS(k_x,k_y,z_s-z_H;\omega)}\hat{P}_{(k_x,k_y,z_H;\omega)}\} \quad (12)$$

2.2 De-noising by wavelet analysis

The wavelet transform has become a standard tool in signal and image processing, and it has found applications in almost all fields of physics, engineering and applied mathematics. In particular, the discrete WT is more appropriate for image de-noising, signal compression and reconstruction, and it is especially popular in the signal processing community.

Let us assume that the noisy image is defined by a set of pixel values $x_{(i,j)}$, where $x(i,j)$ is the pixel coordinate. Then the wavelet transform performed on the array $x_{(i,j)}$ is

$$Wx \quad (13)$$

where W represents the Discrete Wavelet Transform (DWT). The two-dimensional array Wx has the same dimensions as x, and each element $Wx(i,j)$ is a transformed coefficient at coordinate (i,j). In wavelet thresholding, after setting some coefficients to zeros, the reconstructed (de-noised) image is obtained by inverse transformation

$$\hat{x}=W^{-1}(\widehat{Wx}) \quad (14)$$

Suppose we use the mean-square-error (MSE) distortion measure for the empirical risk :

$$D_{mse}(x-\hat{x})=\frac{1}{n}\|\,x-\hat{x}\,\|^2$$
$$=\frac{1}{n}\sum_i\sum_j(x_{i,j}-\hat{x}_{i,j})^2 \quad (15)$$

where n is the total number of image pixels. Furthermore, we use the fact that the Euclidean (L2) norm is invariant to the transformation W, i.e.,

$$D_{mse}(x-\hat{x})=D_{mse}(Wx-\widehat{Wx})$$
$$=\frac{1}{n}\sum_i\sum_j(Wx(i,j)-\widehat{Wx}(i,j))^2 \quad (16)$$

From Eq. (16) it is clear that the sum square of discarded coefficients can be used as a measure of the empirical risk and there is no need to reconstruct the image to compute the empirical risk for each selection of a set of coefficients. In this way, the computational complexity of de-noising with the model selection method can be reduced significantly.

For de-noising applications, the largest-magnitude coefficients are not necessarily the most important because they are contaminated by noise. Furthermore, in either compression or de-noising applications, the wavelet coefficients cannot be coded or ordered strictly according to their magnitudes since they are not statistically independent (in natural images). For good image de-noising, one also needs to specify a 'good' ordering of coefficients reflecting statistical properties of natural images. Meyer(1993), Said and Peralman(1996) showed that the idea of a tree structure originally proposed for image compression can be successfully adapted for de-noising.

Wavelet thresholding for image de-noising

involves two steps : (a) taking the wavelet transform of an image signal (i.e., calculating all the wavelet coefficients); (b) discarding (setting to zero) the coefficients with relatively small or insignificant magnitudes. Each wavelet coefficient here corresponds to a wavelet basis function. So discarding small coefficients is equivalent to discarding wavelet basis functions that have coefficients below a certain threshold. The denoised signal is obtained via inverse wavelet transform of the remaining coefficients. The value of a threshold is usually chosen based on various assumptions about statistical nature of a signal and/or noise. For example, the threshold value derived by Donoho (1994, 1995) under asymptotic assumptions is $T = \sigma \cdot \sqrt{2 \cdot \log(n)}$, where n is the number of samples and σ is the standard deviation of zero-mean Gaussian white noise, which is unknown and needs to be estimated from noisy samples.

3. Robust Nearfield Acoustic Holography Method

The pressure field on a hologram surface ($\xi = \xi_H$) can be expressed as

$$P_{(\xi_1, \xi_2, \xi''_3)} = \iint P_{(\xi'_1, \xi'_2, \xi_3)} G_{HS(\xi_1 - \xi'_1, \xi_2 - \xi'_2)} d\xi'_1 d\xi'_2$$

After impinging the noise field $N_{(\xi_1, \xi_2, \xi''_3)}$ into the pressure field, the noisy pressure field is

$$P'_{(\xi_1, \xi_2, \xi''_3)} = P_{(\xi_1, \xi_2, \xi''_3)} + N_{(\xi_1, \xi_2, \xi''_3)}. \qquad (17)$$

For de-noising the impinged noise field $N_{(\xi_1, \xi_2, \xi''_3)}$ from the noisy pressure field, the wavelet decomposition methodology is required.

Suppose an unknown function P on $[0, 1]$ must be reconstructed from the noisy data

$$P'_{ij} = P_{ij} + N_{ij}, \quad i, j = 0, \dots, n-1 \qquad (18)$$

where N_{ij} is a Gaussian noise.

The goal of de-noising is to minimize the mean-square error

$$D_{mse}(\hat{P} - P) = n^{-1} \|\hat{P} - P\|^2$$
$$= n^{-1} \sum_{i=0}^{n-1} (\hat{P}_{ij} - P_{ij})^2 \qquad (19)$$

subject to the constraint with high probability, $\hat{P}_{ij}$ is at least as smooth as P_{ij}. High probability constraint relates on the observation that whether a wavelet coefficient in a sub-band is lower than a threshold, i.e. it is not significant, then its children on the corresponding wavelet hierarchical tree, located at the same spatial location, are not significance with high probability too.

To satisfy the above mentioned two criteria, i. e., optimization of MSE and the constraint, Donoho and Johnstone (1994) proposed a reconstruction method with a thresholding process for recovering functions from noisy data.

(1) Apply the interval-adapted multi resolution algorithm to the measured data for obtaining empirical wavelet coefficients.

(2) Apply the soft thresholding nonlinearity $\eta_{t(y)} = \mathrm{sgn}(y)(|y| - t)_+$ coordinate-wise to the empirical wavelet coefficients with specially-chosen threshold $t_n = \sqrt{2 \log(n)} \cdot \gamma_1 \cdot \sigma / \sqrt{n}$, where γ_1 is a constant.

(3) Invert the pyramid filtering, recovering $\hat{x}_{n(t_i)}$, $i = 0, \dots, n-1$.

Given that the observed image, P'_{ij}, is modeled as $P'_{ij} = P_{ij} + N_{ij}$ and if the error N_{ij} is Gaussian and uncorrelated (both spatially and with P_{ij}) then finding P_{ij} from P'_{ij} is a classical statistical estimation problem. Since the estimation procedure should work for a variety of signals images $P \in \mathbf{P}$ (where $\mathbf{P}$ is the space set of all images belonging to the application considered), the goal is to find $\hat{P}_{ij}$ such that $\sup_{P \in \mathbf{P}} \|\hat{P}_{ij} - P_{ij}\|$ is minimized. Let W and W^{-1} denote the wavelet and inverse wavelet transform operators, respectively. Then Donoho (1995) showed that spurious oscillations or equivalently smoothness of the signal P_{ij} can be maintained by imposing the shrinkage condition

$$|W\hat{P}_{ij}| \leq |WP_{ij}|. \qquad (20)$$

This problem has a solution which is asymptotically near optimal (simultaneously) for a wide variety of classes $\mathbf{P}$, which is proven by Said and Pearlman (1996). The procedure, $\hat{P}_{ij}$, satisfying the above minimax problem with the given smoothness condition is given by soft-thresholding in the wavelet domain where the threshold depends

on the variance of N_{ij} (the noise). Then the nonlinear wavelet procedure is given by

$$\hat{P}_{ij} = W^{-1} T_\delta (W P_{ij}') \qquad (21)$$

and

$$T_\delta(x) = \begin{cases} x - \text{sgn}(x)\,\delta & for \; |x| > \delta \\ 0 & for \; |x| \le \delta \end{cases} \qquad (22)$$

is the proposed soft-thresholding rule. The threshold δ is obtained by an estimation procedure from the observed image data P_{ij}'.

Imposing the shrinkage condition results in two important qualitative features (i) reconstruction is noise-free in the sense that no spurious oscillations are introduced other than in the data P_{ij}', and (ii) relatively sharp features in P_{ij}' are maintained.

Donoho (1995) showed theoretically that soft-thresholding is the optimal nonlinear function to apply if smoothness of the estimate is important. The optimality of the soft-threshold is in terms of mean squared error subject to smoothness. The threshold, δ, can be formulated as

$$\delta = \lambda \hat{\sigma}_{(P')} \qquad (23)$$

where λ is a constant and $\hat{\sigma}_{(P')}$ is an estimate of the noise standard deviation. Donoho and Johnstone (1994) showed that in fact if $\lambda = \sqrt{2 \log(n)}$ then δ was the optimal minimax threshold subject to the assumptions previously mentioned. Hence the challenge is to design a robust noise variance estimator for any given problem.

4. Numerical Example

In engineering applications, measured data have errors due to random fluctuation or system errors. Even if these errors can be reduced by averaging and calibration, the results are not free from errors. There are many error sources like bias, random errors due to microphone mismatching among microphones and position mismatching.

The goal is to show that wavelet based noise suppression can be used for minimizing the noise impinged on acoustic field measured on a hologram surface. While Wang and Wu (1997)

showed that their algorithm is robust to errors (position error and bias error) with imposed 5% errors to every acoustic measured data, the author superimposed relative errors from 13.7% to 92% based on absolute value of each measured sound pressure level on the original acoustic field and got the clear image of acoustic holography by using the wavelet based on the noise suppression method. It shows that the proposed scheme is good compared with the algorithm proposed by Wang and Wu (1997).

The quality of reconstructed acoustic image should be judged because the image has inevitable errors due to finite hologram in near field acoustic holography. To judge the quality of reconstructed acoustic field, the MAC (Modal Assurance Criterion) is chosen because it is easy to compare the shapes.

$$MAC = \frac{\sqrt{\sum\limits_m \sum\limits_n P_{s(m,n)} P_{a(m,n)}^* \sum\limits_m \sum\limits_n P_{s(m,n)}^* P_{a(m,n)}}}{\sqrt{\sum\limits_m \sum\limits_n P_{s(m,n)}^* P_{s(m,n)} \sum\limits_m \sum\limits_n P_{a(m,n)}^* P_{a(m,n)}}} \qquad (24)$$

In this computer simulation, the wave number is considered as 2π, by making the frequency identical to the speed of sound. The hologram surface is located at 0.3m, and the source plane is 0.01m. The sampling spacing is 0.2m. The number of hologram data is 32 by 32. The simulation works have been done for three cases. The first one is an original image without any corruption. The second image is corrupted by Gaussian and chirping noises. The last one is same as the second one except de-noised by wavelet and thresholding. And the backward propagation process has been applied to obtain the acoustic field image on the source plane. The acoustic images on the hologram surface and source surface have been compared with the original that has one as its MAC value.

The example has two monopole sources at [0.6m, 0.8m] and [-0.8m, 0.4m] with the unit strength.

Two examples of robust NAH are studied with two monopoles. Figures 2 and 3 show that the relative errors in reconstruction of the acoustic field for two monopoles with noisy data. Figure 2
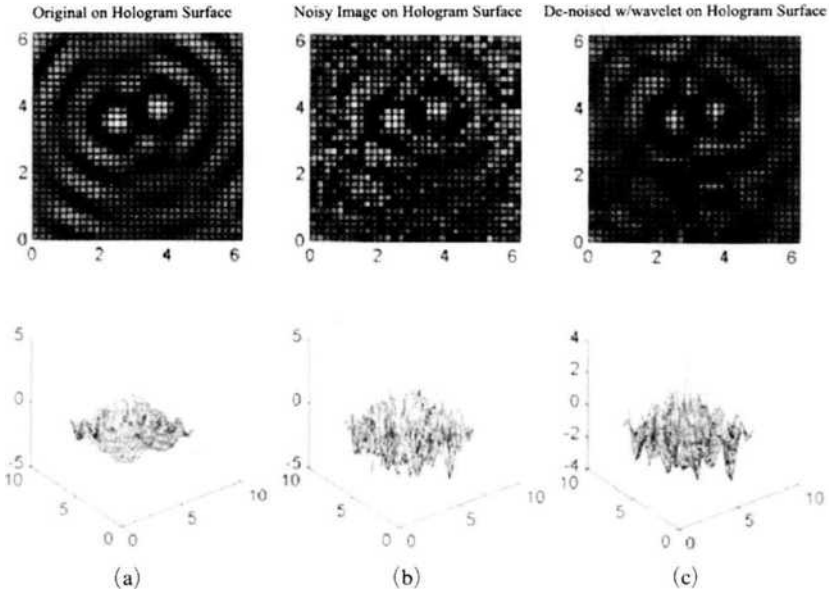
Original on Hologram Surface   Noisy Image on Hologram Surface   De-noised w/wavelet on Hologram Surface

(a)   (b)   (c)

Fig. 2 Acoustic images on hologram surface

Backward with Original Image   Backward with Noisy Imege   Backward with De-noised Image

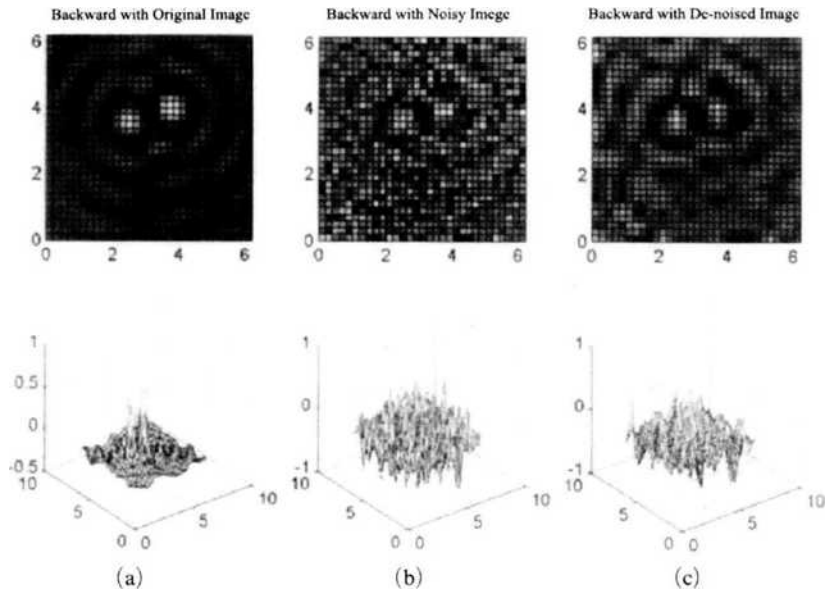(a)   (b)   (c)

Fig. 3 Acoustic images on hologram surface on source plane

(a) denotes an original image on the hologram surface, Fig. 2(b) shows the noisy image corrupted by Gaussian noise and chirping noise and Fig. 2(c) represents the de-noised image by a wavelet scheme.

Figure 3(a) denotes an original image on the prediction surface (source surface), Fig. 3(b) shows the backward propagated image using the noisy image and Fig. 3(c) represents the backward propagated image using the de-noised image by a wavelet scheme.

MAC were calculated for every case in evaluating the quality of acoustic field images. The results are shown in Table 1.

Table 1   MAC in several cases

Cases		MAC
Hologram Surface	Noisy	0.680
	De-noised	0.780
Prediction Surface	Original	0.886
	Noisy	0.476
	De-noised	0.640

Table 2   PSNR in several cases

Cases		PSNR
Hologram Surface	Noisy	47.8
	De-noised	50.7
Prediction Surface	Original	43.8
	Noisy	37.7
	De-noised	40.5

Another judging criterion is the peak-signal-to-noise ratio (PSNR) defined by

$$PSNR = 20 \log_{10} \frac{255}{RMSE} \qquad (25)$$

where for an N by M image, $P_{(i,j)}$, the RMSE (Root Mean Squared Error) is defined by

$$RSME = \sqrt{\frac{1}{N \cdot M} \sum_i \sum_j \{P_{(i,j)} - \hat{P}_{(i,j)}\}^* \{P_{(i,j)} - \hat{P}_{(i,j)}\}} \qquad (26)$$

for complex variables $P_{(i,j)}$ and $\hat{P}_{(i,j)}$.

PSNR is used to evaluate objectively the image quality in image processing communities. The higher value of PSNR means better image reconstruction. The values of PSNR for each case are shown in Table 2.

Based on the MAC and PSNR values for judging quality, it is shown that the acoustic field image is enhanced by wavelet thresholding scheme even if the acoustic field is corrupted by errors or noise on the hologram surface.

5. Conclusions

The NAH with the wavelet de-noising scheme is found to be appropriate to reconstruct an acoustic field on the hologram surface and prediction surface even if the field on the hologram is noisy. This scheme is mainly concerned with inverse acoustics using NAH and wavelet

analysis, that is, reconstruction of the acoustic field on the noise source surface from measured acoustic pressure signals on the hologram surface. The proposed method obtains the de-noised field from noisy field on noise source plane reconstructed through the backward propagation of NAH. It is shown that the scheme is useful for identifying the noise sources on prediction surface through the computer simulation. And it is proven that the scheme is robust to high degrees of uncertainties in the measured data using wavelet de-noising.

References

Borgiotti, G., Sarkissian, A., Williams, E. G. and Schuetz, L., 1990, "Conformal Generalized Near-Field Acoustic Holography for Axisymmetric Geometries," *J. Acoust. Soc. Am.* Vol. 88, pp. 199~209

Chambolle, A., DeVore, R. A., Lee, N. Y. and Lucier, B. J., 1998, "Nonlinear Wavelet Image Processing : Variational Problems, Compression and Noise Removal through Wavelet Shrinkage," *IEEE Trans. Image Proc.*, Vol. 7, pp. 319~335

Chang, S. G. and Vetterli, M., 1997, "Spatial Adaptive Wavelet Thresholding for Image Denoising," *Proc of IEEE Intl Conf on Image Processing*, pp. 374~377

Coifman, R. R. and Donoho, D. L., 1995, *Ideal Translation Invariant De-noising*, Springer Verlag

Donoho, D. L., 1992, "Wavelet Thresholding and W. V. D. : A 10-minute Tour," *Intl. Conf. on Wavelets and Applications*, Toulouse, France, June

Donoho, D. L. and Johnstone, I. M., 1993, "Adaptating to Unknown Smoothness by Wavelet Shrinkage," *Technical Report*, Department of Statistics, Stanford University

Donoho, D. L. and Johnstone, I. M., 1994, "Ideal Spatial Adaptation Via Wavelet Thresholding," *Biometrika*, Vol. 81, pp. 425~455

Donoho, D. L., 1995, "De-Noising by Soft-Threshholding," *IEEE Trans. Info. Theory*, Vol. 41, No. 3, pp. 613~627

Dumbacher, S. M., Brown, D. L., Blough, J. R. and Bono, R. W., 2000, "Practical Aspects of

Making NAH Measurements," *SAE Transaction*, Vol. 108, No. 6, Part 2., pp. 3081~3090

Goodman, W., 1968, *Introduction to Fourier Optics*, McGraw-Hill

Haar, A., 1910, "Zur Theorie Der Orthogonalen Funktionen-Systeme," *Math. Ann.*, Vol. 69, pp. 331~371

Maynard, J. D., Williams, E. G. and Lee Y., 1985, "Nearfield Acoustic Holography : I. Theory of Generalized Holography and the Development of NAH," *J. Acoust. Soc. Am.* Vol. 78, No. 4, pp. 1395~1413

Meyer, Y., 1993, *Wavelets : Algorithms and Applications*, SIAM

Morlet, J., 1983, "Sampling Theory and Wave Propagation," in NATO ASI Series, Vol. 1, *Issues in Acoustic signal/Image processing and recognition*, C. H. Chen, ed. Springer-Verlag, Berlin, pp. 233~261

Said, A. and Pearlman, W. A., 1996, "A New Fast and Efficient Image Codec Based on Set Partitioning in Hierarchical Trees," *IEEE Trans. Circ. and Syst. Video Tech.*, Vol. 6, No. 3, pp. 243~250

Shao, X. and Cherkassky, V., 1998, "Model Selection for Wavelet-Based Signal Estimation," *Proc. IEEE Intl. Joint Conf. on Neural Networks*, Vol. 2, pp. 843~848

Shapiro, J. M., 1993, "Embedded Image Coding Using Zerotrees of Wavelet Coefficients," *IEEE Trans. Signal Processing*, Vol. 41, pp. 3445~3462, Dec.

Simoncelli, E. P., 1999, "Bayesian De-noising of Visual Images in the Wavelet Domain," in *Bayesian Inference in Wavelet Based Models*, Muller and Vidakovic (eds.), Springer Verlag

Verosi, W. D. and Maynard, J. D., 1987, "Nearfield Acoustic Holography : II. Holographic Reconstruction Algorithms and Computer Algorithms," *J. Acoust. Soc. Am.* Vol. 81, No. 5, pp. 1307~1322

Wang, Z. and Wu, S. F., 1997, "Helmholtz Equation-Least-Squares Method for Reconstructing the Acoustic Pressure Field," *J. Acoust. Soc. Am.*, Vol. 102, No. 4, pp. 2020~2032